BMC Plant Biology

RESEARCH

Open Access

Genetic dissection of maize grain moisture content and dehydration rate using high-density bin mapping in a recombinant inbred line population

Jun Zhang[1†], Yingying Zhang[2†], Fengqi Zhang[1], Lei Tian[3], Zhiyan Ma[1], Xiaopan Wu[4], Qingwei Zhou[5], Qianjin Zhang[1], Xinyuan Mu[1], Yanping Fan[1], Laikun Xia[1*] and Yong Ding[1*]

Abstract

Maize (*Zea mays* L.) grain moisture content (GMC) at harvest is a key determinant of seed preservation, grain quality, and drying costs, with the grain dehydration rate (GDR) playing a critical role in determining GMC. This study focused on understanding the genetic basis of GDR by utilizing a recombinant inbred line population of 310 lines derived from PB80 and PHJ65, assessed across three environments with high-density SNP markers. A genetic linkage map spanning 1237.36 cM with 5235 bin markers was constructed, leading to the identification of 23 quantitative trait loci (QTLs) associated with GMC and Area Under the Dry Down Curve (AUDDC) across multiple chromosomes, with several QTLs explaining over 10% of the phenotypic variance. Significant QTLs, including *qGMC1.1*, *qGMC2.2*, and *qAUDDC2.2*, were consistently detected across various environments and developmental stages. Transcriptomic analysis identified 21 candidate genes within these QTL regions, including key transcription factors and metabolism-related genes. These findings contribute to a better understanding of the genetic control of GMC and GDR, may serve as a foundation for future breeding efforts in maize breeding to enhance mechanized production efficiency and reduce post-harvest drying costs.

Keywords Maize, Grain moisture content, Grain dehydration rate, Quantitative trait loci mapping, High-density bin mapping, Recombinant inbred line population, Marker-assisted selection, Transcriptomic analysis

†Jun Zhang and Yingying Zhang contributed equally to this work.

*Correspondence:
Laikun Xia
xialaikun@126.com
Yong Ding
dingyong1974@163.com

[1]Cereal Crops Research Institute, Henan Academy of Agricultural Sciences/Henan Provincial Key Lab of Maize Biology, Zhengzhou 450002, China
[2]Anyang Academy of Agricultural Sciences, Anyang 455000, China
[3]State Key Laboratory of Wheat and Maize Crop Science, Center for Crop Genome Engineering, College of Agronomy, Henan Agricultural University, Zhengzhou 450046, China
[4]Zhengzhou Beiqing Seed Industry Co., Ltd, Zhengzhou 450002, China
[5]Henan Sutai Agricultural Technology Co., Ltd, Zhengzhou 450002, China

Introduction

Maize (*Zea mays* L.) stands as one of the most vital crops globally, not only for its productivity but also for its economic significance. The shift towards whole-process mechanization in agriculture, aimed at reducing production costs and enhancing efficiency, has underscored the critical need to optimize various aspects of maize production. Among these, the dehydration of maize kernels is particularly important, as it directly affects the grain moisture content (GMC) at harvest—a key determinant for mechanical harvesting efficiency, seed preservation, and overall grain quality [1].

Maintaining low GMC is essential to minimizing the costs associated with artificial drying, transportation, and storage of maize [2]. In regions characterized by low temperatures, high humidity, and limited daylight, high GMC poses significant challenges by impeding rapid grain dehydration, increasing the risk of grain spoilage due to mildew, and ultimately leading to substantial economic losses for growers [3, 4]. Even when artificial drying is employed, high GMC can prolong drying times, thereby increasing labor and financial costs [5]. Therefore, optimizing GMC at harvest is of paramount importance, particularly in temperate regions, to ensure the safe and cost-effective production, transport, and storage of maize [6]. Beyond direct agricultural impacts, the optimization of GMC and grain dehydration rate (GDR) holds broader significance for postharvest processing and mechanized agricultural systems. Achieving low GMC at harvest not only reduces the energy and cost demands of artificial drying but also mitigates spoilage risks associated with high moisture, such as fungal contamination, which can compromise grain quality and storage stability [4]. Additionally, in large-scale, mechanized operations, rapid grain dehydration is essential for achieving moisture levels suitable for efficient harvesting and storage, thereby lowering logistical burdens and economic costs [7, 8]. Consequently, enhancing our understanding of GMC and GDR has practical implications, promoting sustainability and efficiency in maize production across diverse agricultural systems.

GMC at harvest is largely determined by two factors: the initial moisture content at physiological maturity and the GDR during the post-maturity drying period [4, 8]. GDR is a critical trait that reflects the rate of moisture loss in maize kernels and is closely associated with final GMC levels. Identifying and selecting maize hybrids that combine low GMC with high GDR is crucial for enabling efficient mechanical harvesting—a key component of modern, mechanized maize production [9, 10]. Over the past decade, significant research efforts have been directed towards understanding the genetic foundations of GMC and GDR. However, the low density of genetic markers in earlier studies has limited the fine-mapping of quantitative trait loci (QTLs) associated with these traits. For example, only *qGwc1.1*, a QTL for grain moisture content, has been successfully fine-mapped to a narrow region using traditional markers [11]. The challenges of accurately measuring GMC and efficiently quantifying GDR have further complicated the identification of genetic loci and their regulatory mechanisms, highlighting the need for more advanced genetic tools and high-efficiency phenotypic indicators [2, 6, 12–17]. In recent years, advances in QTL mapping have shed light on the genetic basis of GMC and GDR, yet many studies remain constrained by the limitations of low marker density, leading to reduced resolution in pinpointing key loci. Recent advancements in high-density genetic mapping techniques, such as genotyping-by-sequencing (GBS), now offer a more refined approach by increasing marker density, enabling more accurate QTL mapping, and facilitating a deeper understanding of the genetic architecture of GMC and GDR [18–20].

In this study, we investigated the genetic and environmental factors influencing GMC and GDR using a recombinant inbred line (RIL) population derived from a cross between PB80 and PHJ65 to provide insights into their underlying regulatory mechanisms. Using a GBS approach, we generated a high-density SNP marker set and constructed a detailed linkage map. This map facilitated the identification of QTLs associated with GMC and GDR across three different environments and developmental stages. Additionally, we integrated QTL mapping with transcriptomic analysis to identify candidate genes involved in grain dehydration. Finally, eight candidate genes were identified. These findings provide insights into the genetic control of maize dehydration traits and may have potential applications in developing maize varieties better suited for mechanized production. Furthermore, this study could contribute to greater efficiency and profitability in maize cultivation.

Materials and methods

Genetic materials and growing conditions

A RIL population comprising 310 lines was developed using the single seed descent method from a cross between two maize lines, PB80 and PHJ65, known for their contrasting dehydration characteristics [21]. PHJ65 exhibits high grain GDR and low final moisture levels, while PB80 has a lower GDR and higher final moisture levels [16]. Both parental lines were publicly released by the National Maize Industry Technical System, ensuring their standardized genetic background and broad accessibility for research and breeding. The RIL population, alongside the parental lines, was grown in three distinct geographical locations in Henan province, China: Xinxiang (E113°97′, N35°05′), Anyang (E114°38′, N36°10′), and Zhoukou (E115°07′, N33°41′) during the summer

season of 2020 and 2021. These locations represent the varied agro-ecological conditions in northern, central, and southern Henan. All the maize lines were designed using a randomized complete block design with one-row plots and two replications. The plants were manually sown in rows of 3.00 m in length, with intra-row spacing of 0.60 m and inter-row spacing of 0.25 m, with a total of 17 plants at a density of 60,000 plants/ha. Standard irrigation and fertilization management were applied throughout the growing period, including to the guard rows.

Determination of GMC and GDR

GMC was assessed for each line at three developmental stages: 35, 45, and 55 days after pollination (DAP), using a portable HB-300 moisture meter (Kett Electric Laboratory). The time points for moisture content measurements were selected in each line multiple times (every ten days) beginning at 35 days after pollination to cover the entire period of kernel development from the early stage to the maturity or post-maturity stage [4, 22]. These stages capture critical dynamics in GMC and GDR for genetic analysis. This analysis allowed us to systematically dissect the dynamics of grain moisture during kernel development. Following the manufacturer's instructions, the moisture meter probes were inserted through the husks into the kernels of the sampled ears. To ensure uniform ear development, both primary and subsequent ears of each line were bagged prior to silk emergence, and pollination was conducted simultaneously across all lines. For each developmental stage, five uniformly grown plants per line were selected, and three replicate measurements were taken from the midsection of the ears. The average value obtained from these measurements was used as the phenotypic value for each line. The mean value derived from two replications was considered as the final phenotypic value for use in QTL mapping.

In addition, the GDR was evaluated using the Area Under the Dry Down Curve (AUDDC) method, which provides an efficient metric for assessing GDR (Yang et al., 2010). A lower AUDDC value corresponds to a higher GDR, indicating more efficient water loss from the grain. The AUDDC was calculated using the formula:

$$AUDDC = \sum_{i}^{n-1} \left[\frac{y_i + y_{i+1}}{2}\right](t_{i+1} - t_i)$$

where n is the number of observations, y is the converted meter reading, i represents the ith rating date, and t is time (in days). Three AUDDC traits were derived based on measurements at three time points: AUDDC1 (35–45 DAP), AUDDC2 (45–55 DAP), and AUDDC (35–55 DAP).

Phenotypic data analysis

For each line, phenotypic measurements were collected from five plants per line across three locations to account for environmental variation. For each developmental stage (35, 45, and 55 days after pollination), the moisture content was recorded from three replicates. The experiment was conducted across three geographically distinct environments in Henan province (Xinxiang, Anyang and Zhoukou) to capture environmental variation. Data analysis was performed using analysis of variance (ANOVA), examining the effects of genotype, environment, and genotype × environment interactions. Broad-sense heritability was also calculated to assess the genetic contribution to these traits. Statistical analysis was conducted using the AOV tool in IciMapping software (version 4.2; http://www.isbreeding.net) and IBM SPSS Statistics. The best linear unbiased predictors (BLUPs) were estimated using META-R software for multi-environment analysis [23].

DNA extraction, library preparation, and sequencing

Total genomic DNA was extracted from fresh leaf samples of the two parental lines and 310 RIL individuals using a Plant Genomic DNA kit (TIANGEN, Beijing, China). The DNA purity and concentration were assessed using a NanoPhotometer® spectrophotometer (IMPLEN, CA, USA) and a Qubit® 2.0 Fluorometer (Life Technologies, CA, USA). DNA integrity and quality were evaluated via 1% agarose gel electrophoresis. Qualified DNA samples were then digested, sequenced, purified, and PCR-amplified to complete the library preparation process. Illumina paired-end libraries of 300–500 bp were constructed for the 310 RILs and the two parental lines. Paired-end sequencing of selected tags was performed using a NovaSeq6000 high-throughput sequencing platform at the Novogene Bioinformatics Institute, Beijing, China.

To ensure data reliability and minimize bias, raw fastq data were processed through a series of quality control (QC) steps using custom in-house scripts. QC criteria included: (1) removal of reads with ≥ 10% unidentified nucleotides (N), (2) discarding reads where 50% of bases had Phred scores of < 5, (3) including reads with > 10 nucleotides aligned to the adapter, allowing ≤ 10% mismatches, and (4) eliminating reads containing cut site remnant sequences. High-quality clean data were obtained following stringent filtering. These clean reads were aligned to the maize reference genome using BWA software [24]. Population SNP detection was performed using SAMtools software [25]. A Bayesian model was employed to identify polymorphic sites within the population, and subsequent filtering and screening yielded high-quality SNPs, which were then annotated using ANNOVAR [26].

Bin map construction and QTL analyses

A bin map for this study was constructed using the Maximum Parsimonious Inference of Recombination (MPR) method [27]. The key steps are as follows: Initially, SNPs were identified to define the genotypes of the parental lines, PB80 and PHJ65, with an emphasis on maximizing the use of available SNP information. To ensure high data quality, SNPs of lower quality were then filtered out through permutation resampling of SNP windows and Bayesian inference. Subsequently, genotyping of the RIL population was performed using high-quality SNPs, with error correction applied via a hidden Markov model (function: correctGeno; parameter: "correctFUN = correctFUNHMM"; error rate: 0.0103). Finally, consecutive SNPs sharing the same genotype from one parent were grouped into bins using a sliding window approach (function: genoToBin). The window size was set at 500 kb, with a minimum of 20 SNPs per window, and the bins shorter than 100 kb or containing fewer than 20 SNPs were considered incomplete and were excluded from further analysis.

QTL analyses were conducted using QTL IciMapping version 4.2 software [28]. The QTL scan was performed with a 1 cM interval and an LOD threshold of 2.5. To minimize the loss of QTLs with small effects, LOD thresholds were empirically set to 2.5, following previous studies [5, 11, 29]. QTLs identified in multiple environments and located within overlapping 1.5-LOD confidence intervals (as provided by the software) were considered identical [30]. QTLs consistently detected across environments and accounting for over 10% of the phenotypic variation were classified as major QTLs [31]. Initial QTL mapping was conducted separately for each of the three field trials, integrating data from two replicates to capture all potential QTLs. Additionally, the BLUP method was applied to predict the trait expectation for each RIL across the three trials, supporting comprehensive QTL mapping [11].

Candidate gene prediction

Based on the physical positions of SNP markers flanking each QTL, physical intervals were defined. Genes within these intervals were predicted using the MaizeGDB database (https://maizegdb.org/) to identify corresponding protein sequences. The predicted protein sequences were then aligned with those in the National Center for Biotechnology Information (NCBI) database (http://blast.ncbi.nlm.nih.gov/) to analyze homologous proteins in other species, suggesting potential biological functions of these genes in Arabidopsis and rice.

Transcriptomic analysis for parental RNA isolation

Kernel tissues from PB80 and PHJ65 were collected at 35, 45, and 55 days after pollination (DAP) during kernel development. The tissues were immediately frozen in liquid nitrogen and stored at -80 °C. Three biological replicates were established for each stage. Total RNA was extracted following the manufacturer's instructions using a Plant RNA Purification Kit (Tiangen, Beijing, China). RNA sequencing was conducted using the Illumina NovaSeq-PE150 Platform at Novogene (Novogene Co., Ltd., Tianjin, China). Sequencing reads were quality-trimmed using Trimmomatic 0.38, with low-quality reads removed. High-quality reads were aligned to the maize B73 reference genome (RefGen_v4; sequence assembly http://ftp.ensemblgenomes.org/pub/plants/release-41/fasta/zea_mays/dna/) using HISAT2 version 2.0.5. Gene expression levels were normalized and quantified as fragments per kilobase of transcript per million mapped reads (FPKM) using StringTie version 1.3.5 (https://ccb.jhu.edu/software/stringtie). Differentially expressed genes (DEGs) were identified using edgeR, based on a false discovery rate (FDR)-adjusted P-value ≤ 0.05 and fold changes ≥ 2 or ≤ 0.5. Functional and pathway enrichment analysis was performed using the OmicShare tools, a free online platform for data analysis (www.omicshare.com/tools).

Results

Construction of a high-density bin map confirms robust collinearity and accurate recombination rates

The genetic linkage map was constructed using 2,218,988 high-quality, biallelic, homozygous SNP markers identified between the parental lines PB80 and PHJ65 (Fig. 1A; Table 1, Figure. S2). These markers were processed using a sliding window approach, resulting in 5,235 bin markers. The length of the bin markers mainly ranged from 100 kb to 400 kb, with an average physical interval of 404.70 kb between adjacent bins (Table 1, Figure. S1A). The final genetic map spanned 1,237.36 centiMorgans (cM) across 10 linkage groups (LGs), with an average of 523 bin markers per chromosome. Chromosome 1 contained the most bin markers (821), while chromosome 10 contained the fewest (345). Chromosome lengths ranged from 99.56 cM (chromosome 10) to 183.44 cM (chromosome 1), and the overall map density was 4.23 bins per cM (Table 1). The genetic distance between neighboring bins was approximately 0.25 cM, mainly ranging from 0.0 to 1.25 cM (Figure. S1B). Collinearity analysis confirmed strong alignment between genetic and physical positions on the reference genome, ensuring accurate recombination rate calculations (Figure. S3B, C). Pairwise recombination fractions indicated no significant anomalies, validating the map's suitability for downstream QTL analysis (Fig. S1B).

Table 1 Summary statistics of the genetic linkage map for the RIL population

Linkage group	Number of SNPs	Number of bins	Genetic distance (cM)	Average bins/cM	Average distance (cM)	Average length of bin (kb)	Recombination rate (cM/Mb)	< 5 cM Gap	Max. gap (cM)
LG1	23,346	821	183.44	4.48	0.22	373.95	0.6	821	1.76
LG2	22,100	632	132.86	4.76	0.21	386.73	0.54	632	2.10
LG3	18,797	576	132.58	4.34	0.23	409.06	0.56	576	1.38
LG4	18,826	527	124.73	4.27	0.24	468.58	0.5	527	2.30
LG5	15,924	530	124.25	4.23	0.23	422.09	0.55	530	1.95
LG6	13,281	483	109.36	4.27	0.23	360.09	0.63	483	3.27
LG7	15,880	449	109.53	4.10	0.24	406.17	0.6	449	2.27
LG8	11,754	429	105.51	4.07	0.25	422.17	0.58	429	2.09
LG9	12,538	443	115.54	3.83	0.26	360.60	0.72	443	1.93
LG10	13,332	345	99.56	3.47	0.29	437.58	0.66	345	2.33
Total	165,778	5235	1237.36	4.23	0.24	402.25	0.594	5235	3.27
Average	16577.8	523.5	123.74	4.23	0.24	404.70	0.594	523.5	2.14

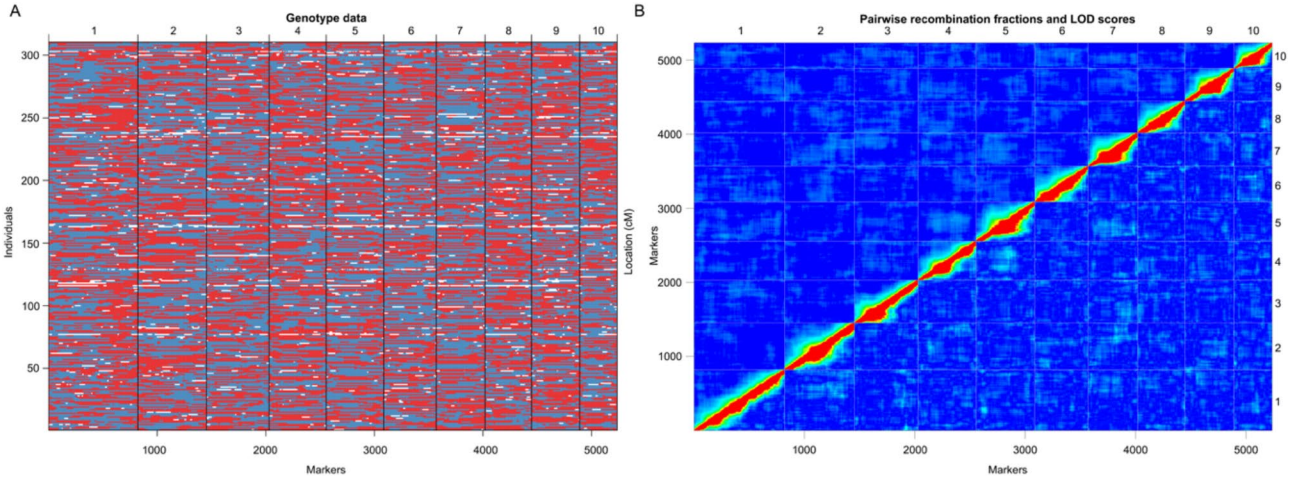

Fig. 1 Whole-genome bin construction in RIL population. **(A)** The bin map of the RIL population. Each column represents a RIL. red indicates PB80 genotype, blue is PHJ65 genotype, and white shows heterozygote. **(B)** Pairwise recombination fractions of bins. The upper left shows recombination fractions between bin pairs, while the lower right displays the logarithm (base 10) of odds (LOD) scores from linkage testing. The primary alignment of signals along the diagonal line suggests a well-constructed bin map

Significant phenotypic variation in GMC and AUDDC reflects genetic diversity and environmental influence

GMC and the AUDDC were measured at three developmental stages across three distinct environments to evaluate phenotypic variation within the RIL population. The parental lines, PB80 (P1) and PHJ65 (P2), exhibited significant differences in GMC and AUDDC across all environments ($p < 0.01$) (Fig. 2). The result showed that PB80 consistently exhibits higher GMC and AUDDC values compared to PHJ65.

The RIL population displayed transgressive segregation, with several lines surpassing the parental GMC levels. As kernel development advanced, average GMC decreased from 31.84 to 18.60%, while the coefficient of variation (CV) increased from 6.25 to 12.04%. A parallel trend was observed for AUDDC, where the average value increased from 287.09 to 508.06, and the CV rose from 6.49 to 9.39% (Table 2). This increase in phenotypic variation over time was attributed to differential dehydration rates among the RILs (Fig. 3). Shapiro-Wilk normality tests confirmed that GMC and AUDDC data approximated normal distributions across all environments and BLUPs (Table 2, Table S1), consistent with the distribution curves typical of quantitative traits (Fig. 3, Figure S4). Analysis of variance (ANOVA) revealed significant effects of genotype, environment, and genotype × environment interactions on GMC and AUDDC (Table S2), with broad-sense heritability estimates ranging from 0.75 to 0.89 for GMC and from 0.82 to 0.85 for AUDDC (Fig. 4, Table S1). These findings indicate a genetic basis for these traits while also highlighting the significant influence of environmental factors.

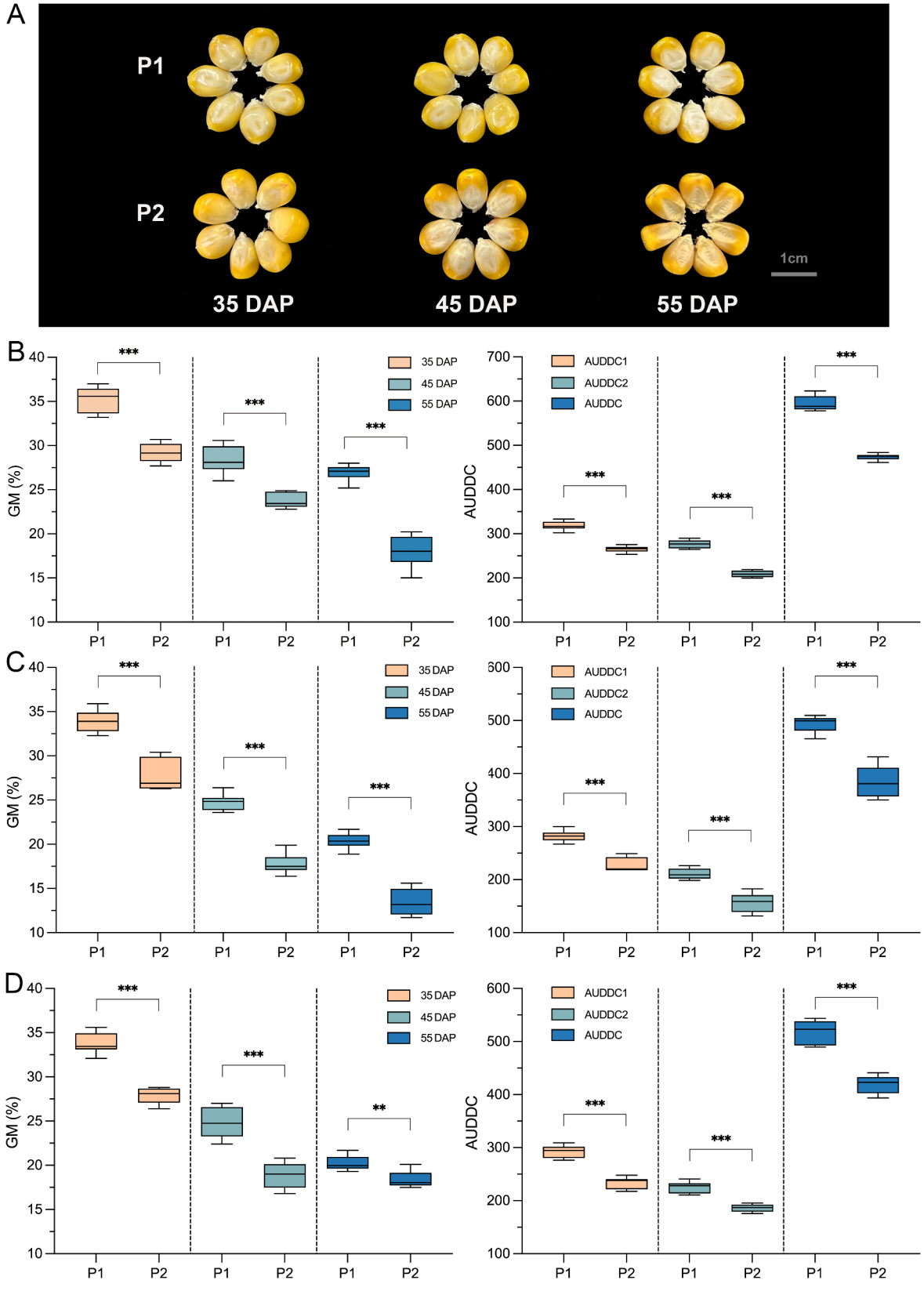

Fig. 2 Comparison of morphological and grain moisture traits among parents "PB80 (P1)", "PHJ65 (P2)". (**A**) Kernel morphology comparison between PB80 and PHJ65. (**B-D**) Boxplots showing differences in grain moisture content (GMC) and area under the drying curve (AUDDC) between parents across three locations: Anyang (**B**), Xinxiang (**C**), and Zhoukou (**D**). Asterisks ("*") indicate highly significant differences between parents based on independent samples t-tests (***$p < 0.001$, **$p < 0.01$)

Table 2 Description of phenotype analysis for GMC and AUDDC in the RIL population (BLUP value)

Trait	Stage	Parents		RIL population			Normality analysis		
		Male	Female	Mean ± SD	Rang	CV (%)	Skew[a]	Kurt[b]	W[c] (*p* value)
GMC	35DAP	34.35 ± 2.33	28.31 ± 1.75	31.84 ± 1.99	23.98–42.16	6.25%	0.49	0.9	0.969(0.000)
	45DAP	26.07 ± 1.57	20.3 ± 1.81	25.55 ± 2.38	15.43–32.37	9.32%	-0.65	1.37	0.975(0.000)
	55DAP	22.43 ± 2.28	16.51 ± 1.81	18.60 ± 2.24	9.14–24.56	12.04%	-0.14	0.58	0.993(0.032)
AUDDC	35-45DAP	292.27 ± 14.1	242.31 ± 15.26	287.09 ± 18.64	225.99-357.16	6.49%	-0.23	1.65	0.978(0.000)
	45-55DAP	241.04 ± 14.43	183.4 ± 12.46	220.83 ± 20.74	133.99-282.51	9.39%	-0.33	0.83	0.990(0.035)
	35-55DAP	533.3 ± 23.33	425.7 ± 24.67	508.06 ± 37.61	342.18-632.26	7.40%	-0.33	1.58	0.982(0.001)

[a] Kurt, kurtosis

[b] Skew, skewness

[c] W, Shariro–Wilk statistic value

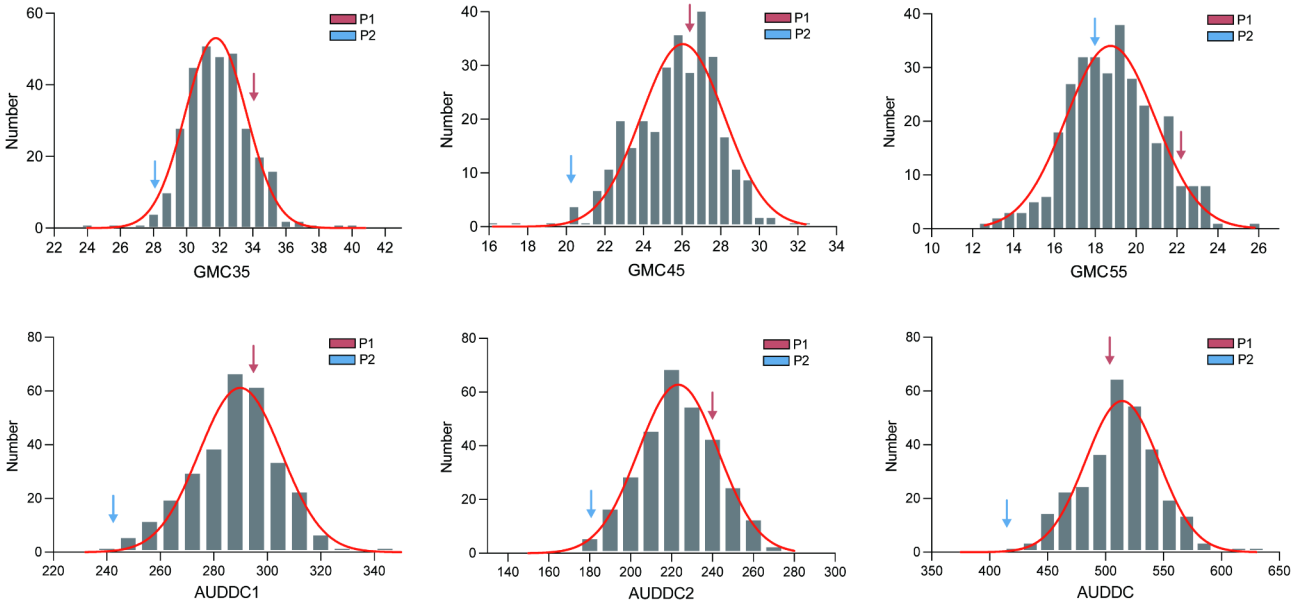

Fig. 3 The phenotypic distribution of grain moisture content (GMC) and dehydration rate (AUDDC) for the RILs at different time points from BLUP value analysis in three field trials. Arrows indicate groups with GMC and AUDDC values similar to those of the parents (P1: PB80 and P2: PHJ65). Red lines represent theoretical normal distribution curve

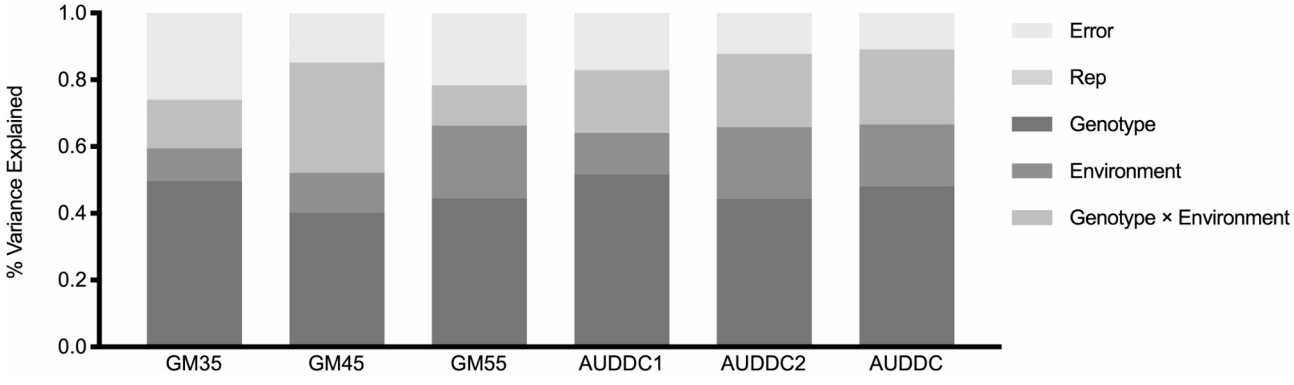

Fig. 4 Variation in GMC35, GMC45, GMC55, AUDDC1, AUDDC2 and AUDDC was attributed to genetic and environmental factors across the RIL population. The different shades of grey in the stacked bar diagram in the stacked bar diagram indicated the various factors that explain phenotypic variance

Consistent identification of key QTLs for GMC and AUDDC across multiple environments

QTL mapping was performed using the inclusive composite interval mapping (ICIM) method, resulting in the identification of 23 QTLs associated with GMC and AUDDC—9 for GMC and 14 for AUDDC—across three environments (Table 3). The GMC QTLs were located on chromosomes 1, 2, 5, 6, 9, and 10, while AUDDC

Table 3 The common QTL related to GMC and AUDDC in three field trials

QTL	Chr	Field trial[a]	DAP	Flanking SNPs	Physical Location (Mb)	LOD	R^{2b}	AE[c]
qGMC1.1	1	XX	35	chr1_194244018-chr1_194374619	194.24-194.37	6.96	8.75	0.46
		AY	35			8.68	10.72	2.57
		ZK	35			4.26	5.80	0.50
qGMC1.2	1	AY	45	chr1_290312240-chr1_290401547	290.31–290.40	5.69	6.59	0.60
qGMC2.1	2	AY	35	chr2_11625725-chr2_11658780	116.26-116.59	4.42	5.11	-0.44
		ZK	35			3.40	4.63	-0.45
qGMC2.2	2	AY	35	chr2_212831691-chr2_213913274	212.83-213.91	5.90	8.02	-1.89
		AY	55			10.31	13.66	-5.57
		ZK	45			9.75	12.98	-3.54
qGMC5.1	5	XX	55	chr5_8089739-chr5_8237769	8.09–8.24	3.66	6.26	0.61
qGMC5.2	5	XX	45	chr5_82543758-chr5_82809360	82.54–82.81	3.04	6.48	0.41
qGMC6.1	6	AY	35	chr6_36034446-chr6_38134067	36.03–38.13	11.27	14.68	-5.20
		XX	35			4.32	4.97	-0.48
qGMC6.2	6	AY	45	chr6_134177797-chr6_134879403	134.18-134.88	3.96	4.55	0.49
qGMC10	10	XX	35	chr10_2218596-chr10_2237123	2.22–2.24	3.31	4.00	0.42
qAUDDC1.1	1	AY	35–45	chr1_35333078-chr1_35973365	35.33–35.97	2.57	3.63	3.30
		ZK	35–45			3.02	4.42	4.21
qAUDDC1.2	1	XX	35–45	chr1_194244018-chr1_194374619	194.24-194.37	6.41	8.88	13.77
		ZK	35–45			9.42	12.58	33.75
qAUDDC1.3	1	AY	35–45	chr1_270704541-chr1_271018694	270.70-271.02	3.21	4.56	3.81
qAUDDC1.4	1	AY	35–55	chr1_290312240-chr1_290401547	290.31–290.40	3.63	4.54	10.57
		AY	45–55			3.17	4.01	6.99
qAUDDC2.1	2	XX	35–45	chr2_26169676-chr2_26861155	26.17–26.86	5.88	7.87	-5.01
qAUDDC2.2	2	XX	35–55	chr2_212831691-chr2_213913274	212.83-213.91	13.73	18.15	54.29
		XX	35–45			9.02	11.46	30.55
		ZK	45–55			6.01	8.14	14.89
qAUDDC3	3	AY	35–55	chr3_231158054-chr3_231225890	231.16-231.23	2.62	3.77	-8.77
		AY	45–55			2.66	3.38	-6.28
qAUDDC4.1	4	AY	35–45	chr4_190313976-chr4_190332634	191.30-190.33	2.73	3.86	-3.38
qAUDDC4.2	4	AY	35–55	chr4_206345467-chr4_206685902	206.35-206.69	3.55	4.45	-10.21
		AY	45–55			2.60	3.68	-6.17
qAUDDC5	5	XX	35–55	chr5_82543758-chr5_82809360	82.54–82.81	3.61	4.14	9.31
qAUDDC6.1	6	AY	35–55	chr6_134177797-chr6_134879403	134.18-134.88	2.86	3.58	9.18
qAUDDC6.2	6	AY	45–55	chr6_145405296-chr6_145506072	145.41-145.51	3.05	3.88	6.71
qAUDDC10.1	10	XX	35–55	chr10_2218596-chr10_2237123	2.22–2.24	2.85	3.11	8.24
		XX	35–45			3.11	3.62	3.64
qAUDDC10.2	10	XX	35–55	chr10_133859005-chr10_134030377	133.86-134.03	3.20	4.13	8.73

[a] XX, Xinxiang; AY, Anyang; ZK, Zhoukou

[b] Coefficient of determination: percentage of phenotypic variance explained by the QTL

c Additive effects of QTLs with a negative sign indicate the contribution of the parent, PB80, while positive values indicate the contribution of the parent, PHJ65

QTLs were distributed across chromosomes 1, 2, 3, 4, 5, 6, and 10. The phenotypic variance explained by individual QTLs ranged from 3.11 to 18.15%, with LOD scores between 2.51 and 13.73. Among these QTLs, 16 trait-enhancing alleles—6 for GMC and 10 for AUDDC—originated from PHJ65, while the remaining 7 alleles—3 for GMC and 4 for AUDDC—were derived from PB80.

Two major GMC-related QTLs, *qGMC1.1* and *qGMC2.2*, were consistently detected across all environments and developmental stages, explaining between 5.80% and 13.66% of phenotypic variance. Additionally, two other QTLs, *qGMC2.1* and *qGMC6.1*, were identified in two environments, contributing 4.63–14.68% of the GMC variance. For AUDDC, the major QTL *qAUDDC2.2* was consistently observed across environments and developmental stages, accounting for 8.14–18.15% of the phenotypic variation. Five other AUDDC QTLs—*qAUDDC1.1*, *qAUDDC1.2*, *qAUDDC1.4*, *qAUDDC3*, *qAUDDC4.2*, and *qAUDDC10.1*—were detected in multiple environments, each explaining 3.11–12.58% of the variance. Notably, two GMC QTLs, *qGMC1.1* and *qGMC2.2*, overlapped with AUDDC QTLs *qAUDDC1.2* and *qAUDDC2.2*, respectively, suggesting a shared genetic basis for these traits. The best linear unbiased

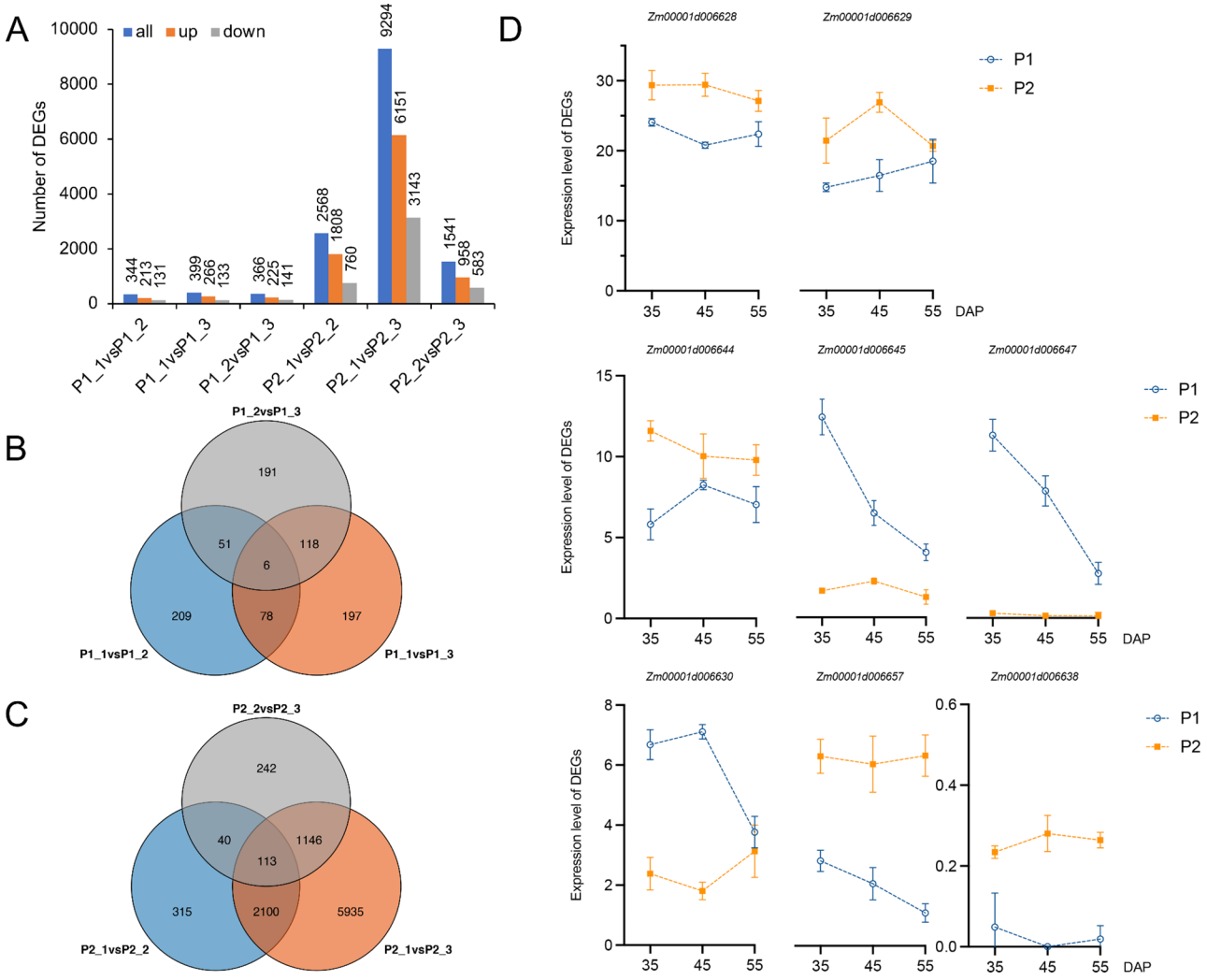

Fig. 5 Transcriptome analysis of parental lines PB80 and PHJ65. (**A**) Number of differentially up- and down-regulated genes at 35-, 45-, and 55-days post-pollination in PB80 and PHJ65. (**B-C**) Venn diagram analysis of differentially expressed genes in PB80 (**B**) and PHJ65 (**C**) at 35-, 45-, and 55-days post-pollination; (**D**) Expression levels of the differentially expressed genes located within QTL regions. "_1," "_2," and "_3" represent 35, 45, and 55 DAP, respectively; "P1" and "P2" refer to PB80 and PHJ65, respectively

prediction (BLUP) model, used to estimate GMC and AUDDC at 35, 45, and 55 days after pollination (DAP) across environments, confirmed the stability of these QTLs in different field conditions.

Transcriptomic analysis correlates differential gene expression with dehydration rates

To further investigate the genetic basis of GMC and dehydration rate (GDR), transcriptomic analysis was performed on seeds from the parental lines PB80 and PHJ65 at 35, 45, and 55 DAP. RNA sequencing revealed significant differential gene expression between the two parental lines. In PHJ65, which exhibited faster dehydration rates, 958 and 6,151 genes were upregulated at 45 and 55 DAP, respectively, compared to PB80, which had fewer upregulated genes (Fig. 5A-C). The analysis identified 5,935 differentially expressed genes (DEGs) between 55 and 45 DAP in PHJ65, indicating a potential correlation between dehydration speed and transcriptomic changes (Fig. 5C). These findings highlight key genes potentially driving the differences in dehydration rates and subsequent GMC in maize.

To explore the physiological processes underlying GMC and GDR, we conducted Gene Ontology (GO) and Kyoto Encyclopedia of Genes and Genomes (KEGG) pathway enrichment analyses on the DEGs identified between the parental lines PB80 and PHJ65. These analyses revealed significant enrichment of DEGs in functional categories related to metabolic processes and amino acid biosynthesis (Figure S5). Notably, DEGs expressed during the development of PB80 seeds were enriched in rhythmic processes (Figure S5A-B), suggesting possible mechanisms by which kernels regulate moisture content and enhance dehydration efficiency. Additionally, DEGs

were associated with pathways involving metabolism, DNA replication, and sugar biosynthesis and degradation. The KEGG terms for circadian rhythm and plant hormone signal transduction were identified during the developmental stages of PB80 and PHJ65 seeds, respectively (Figure S5C-D), suggesting the association between regulatory pathways and the drying process as kernels mature.

Co-localization of QTLs on chromosome 2 identifies 21 candidate genes for GMC and GDR

The stable major QTLs *qGMC2.2* and *qAUDDC2.2* were co-localized within a 81.6 kb region on chromosome 2 (212,831,691–212,913,274 bp), indicating a potential shared genetic basis for both GMC and GDR. Homologous alignment and functional annotation within this region identified 21 candidate genes (Table S4). These genes were categorized into four functional groups: transcription factors, protein-related genes, metabolic process-related genes, and other biological processes. Group 1 included transcription factors such as zinc finger protein *ZAT2* (*Zm00001d006647*) and ethylene-responsive transcription factor *ERN1* (*Zm00001d006653*). Group 2 comprised protein-related genes, including subtilase family protein (*Zm00001d006669*). Group 3 involved genes related to fatty acid metabolism (*Zm00001d006630*), amine metabolism (*Zm00001d006638*), and other metabolic processes. Group 4 consisted of genes involved in various other biological processes. Notably, 8 of these genes (*Zm00001d006628*, *Zm00001d006629*, *Zm00001d006630*, *Zm00001d006638*, *Zm00001d006644*, *Zm00001d006645*, *Zm00001d006647*, *Zm00001d006657*) showed significant differential expression between PB80 and PHJ65, suggesting their involvement in key processes such as protein synthesis, metabolism, circadian rhythm regulation, and DNA transcription (Fig. 5D). These candidate genes may provide a valuable foundation for future research aimed at improving GMC and GDR in maize.

Discussion

Advancing mechanized maize harvesting through genetic optimization of grain moisture content and dehydration rates

Mechanized harvesting is crucial for modern agriculture, as it enables large-scale, efficient, and cost-effective production. However, high GMC at harvest poses significant challenges, including increased energy and drying costs, as well as a higher risk of grain spoilage during storage, leading to substantial economic losses [32]. This challenge is particularly acute in regions with unfavorable climatic conditions for natural grain drying. To address these issues requires the development of maize (*Zea mays* L.) varieties with lower GMC and faster GDR, which are critical for optimizing mechanized harvesting and reducing post-harvest processing costs.

Our study contributes to addressing this challenge by focusing on the genetic improvement of two key traits: GMC and grain GDR. These traits are critical not only for determining the optimal harvest time but also for minimizing post-harvest processing costs and ensuring high-quality grain that resists spoilage. By utilizing advanced, such as high-density bin mapping and GBS, we have made significant strides in identifying the genetic loci that control these traits. The integration of these genetic tools into breeding programs provides potential targets for MAS, which could facilitate the development that are better suited for mechanized harvesting. The identification of stable QTLs and candidate genes associated with GMC and GDR provides potential targets for MAS, which may facilitate the development of maize hybrids with improved drying characteristics. These advancements are especially relevant in the context of global climate change, where variations in weather patterns exacerbate challenges associated with grain drying and storage [33].

Additionally, molecular marker-assisted selection (MAS) allows breeders to incorporate these desirable traits more efficiently and accurately into breeding lines. This precision breeding approach shortens breeding cycle and ensures that maize varieties possess the optimal traits for mechanization [34]. By reducing GMC at harvest and enhancing GDR, we can significantly reduce reliance on artificial drying methods, thus lowering energy consumption and the carbon footprint of maize production. In a broader context, this genetic innovation contributes to the sustainability of maize production systems by enhancing resource use efficiency and reducing the environmental impact of post-harvest processing. As global maize demand increases for food, feed, and industrial applications, the development of mechanization-friendly maize varieties will be crucial in meeting this demand sustainably [35].

In summary, our study contributes to the understanding of the genetic basis of GMC and GDR in maize and identifies potential genetic targets that may aid in improving mechanized maize harvesting. By harnessing genetic innovation, we can pave the way for a new era of maize breeding, focused on efficiency, sustainability, and resilience in the face of evolving agricultural challenges.

High-density bin mapping revolutionizes QTL mapping precision

Linkage analysis has long been an essential tool for deciphering the genetic architecture of quantitative traits in crops [36]. However, traditional QTL mapping approaches have been constrained by limited resolution and low marker density, resulting in broader QTL

intervals and less precision [2, 6, 12, 37, 38]. The advent of high-throughput sequencing technologies, including GBS, has significantly advanced QTL mapping by enabling the generation of dense polymorphic markers, such as SNPs and InDels, which greatly improve mapping efficiency and accuracy in maize [10, 11, 14, 39, 40].

In this study, we utilized GBS approach to develop a RIL population and construct a high-density genetic linkage map. This map included 5,235 bin markers derived from 2,218,988 high-quality SNPs, spanning 1,237.36 cM with an average genetic distance of 0.24 cM between adjacent markers. The mean physical distance between markers was 402.25 kb, and the smallest QTL interval was approximately 100 kb, representing a substantial improvement in resolution compared to previous studies [16]. The high marker density and strong collinearity with the reference genome confirm the map's suitability for precise QTL identification and gene discovery (Figure S2). This advancement in mapping precision is crucial for uncovering the genetic basis of complex traits, such as GMC and GDR.

Precision phenotyping is key to unraveling complex traits

Accurate phenotypic data are critical for effective QTL mapping, especially for complex traits like GMC and GDR, which are influenced by both genetic and environmental factors. The dehydration process from physiological maturity to harvest directly impacts final seed moisture. However, determining the precise timing of physiological maturity is often challenging due to environmental variability. Therefore, we measured GMC at multiple time points beginning at 35 DAP to cover the entire period of kernel development from early to post-maturity stages [4, 10]. This approach allowed us to generate time-series data that were transformed into AUDDC values, providing a comprehensive measure of dehydration rate and other features influencing final grain moisture.

To ensure the accuracy of our phenotypic data, we implemented several stringent methodological controls: (1) pollination dates were adjusted according to the flowering time of materials to ensure synchronized grain filling and dehydration processes; (2) primary and subsequent ears were bagged prior to silk emergence to synchronize ear development across all lines; (3) moisture content was measured by deeply probing kernels with a moisture meter, ensuring that the bract of the ear remained intact and that natural dehydration was not disturbed. These methods have proven effective in obtaining accurate and reliable phenotypic data for QTL mapping [4, 6, 16, 41–46].

Field trials across multiple environments allowed us to assess the QTL stability and consistency under different environmental conditions. The identification of several consistent QTLs across environments supports the robustness of our phenotypic data and the reliability of the mapped QTLs. Notably, QTLs such as *qGMC1.1* and *qAUDDC1.2*, as well as *qGMC2.2* and *qAUDDC2.2*, were co-localized, suggesting that these regions may contain genes that influence GMC and GDR. The positive correlation between GMC and AUDDC (Figure S4) further supports the existence of common genetic loci affecting both traits, offering new opportunities for simultaneous improvement of GMC and GDR in breeding programs [47]. One possible explanation for this co-localization is that this genomic region may contain regulatory elements or genes integral to fundamental processes, such as water transport and cellular homeostasis, that simultaneously affect both traits. To our knowledge, this finding represents a novel insight within maize genetics, as previous research has largely identified separate loci associated with either GMC or GDR, without emphasizing regions that impact both. This discovery underscores the potential of chromosome 2 as a promising target for MAS and simultaneous improvement of GMC and GDR in maize breeding programs. Future studies should aim to elucidate the precise mechanisms within this region to further understand how shared pathways influence these traits, offering a valuable foundation for developing maize varieties optimized for rapid dehydration and low moisture retention.

Deciphering the genetic architecture: key insights into GMC and GDR

The genetic architecture of GMC and GDR is complex, as evidenced by the identification of 23 QTLs in this study, including those detected across multiple environments and developmental stages. Notably, key QTLs such as *qGMC2.2* and *qAUDDC2.2* were consistently detected, suggesting their potential as important loci for breeding programs aimed at reducing GMC and enhancing dehydration rates. The co-localization of these QTLs on chromosome 2 suggests that a single genetic region may influence both traits, which could facilitate breeding efforts by targeting these loci for MAS. However, while these loci showed stability across different environments, additional validation in independent populations and under broader environmental conditions is necessary to confirm their utility in breeding applications. The stable identification of *qGMC2.2* and *qAUDDC2.2* across various environmental conditions makes them particularly attractive candidates for MAS, as their consistent effect on GMC and GDR suggests resilience to environmental variation. By incorporating these loci into MAS strategies, breeders could efficiently develop maize lines with optimized dehydration rates and lower harvest-time moisture content, which are essential for reducing post-harvest drying costs and preventing spoilage

during storage. Future studies would focus on fine mapping these consistent QTL and cloning these genes.

Seed dehydration from the phase of reserve accumulation to maturation drying is associated with distinct gene/protein expression and metabolic switches [48]. The overlap of several QTLs with clusters of DEGs suggests that these genes work in concert to regulate moisture dynamics, aligning closely with the observed phenotypic variation in GMC and GDR. In addition, we further identified eight candidate genes within these QTL regions, providing valuable insights into the molecular mechanisms driving GMC and GDR. These genes, involved in processes such as protein synthesis, metabolism, and circadian regulation, are likely key drivers of seed maturation and dehydration. Notably, *ZAT2* and *ERN1* are transcription factors involved in abiotic stress responses, suggesting they may help kernels modulate internal moisture under variable field conditions [49, 50]. Moreover, genes associated with lipid and amine metabolism indicate possible roles in facilitating water loss through cellular structural changes or osmotic regulation, which could impact grain dehydration rates directly [51]. The identification of *Zm00001d006628*, known as TIME FOR COFFEE (TIC), as a candidate gene associated with GDR is particularly noteworthy. TIC is a key regulator of circadian rhythms and has been implicated in controlling metabolic processes that are essential for seed viability and crop yield [52–54]. The role of TIC in regulating dehydration underscores the importance of circadian mechanisms in seed development and presents a promising target for genetic improvement in maize. Future research should prioritize functional validation of candidate genes within these QTL regions, as well as testing in independent populations and under diverse environmental conditions to confirm their utility for breeding.

Towards a new era of maize breeding: harnessing genetic insights for mechanization

This study provides new insights into the genetic basis of GMC and GDR, traits that are pivotal for mechanized maize harvesting. The development of maize hybrids with optimized GMC and enhanced GDR provides significant benefits for mechanized agriculture by reducing post-harvest costs and improving efficiency [55]. Low-GMC, high-GDR hybrids may lessen the reliance on artificial drying, which is a major cost in maize production, allowing producers to save on fuel and electricity. For large-scale operations, this reduction in drying requirements can significantly enhance profitability, especially in areas with limited drying infrastructure. Additionally, the decrease in energy consumption supports sustainable agricultural practices by lowering the carbon footprint of maize production, making these hybrids ideal for eco-friendly farming systems. Furthermore, these genetic improvements have the potential to enhance maize adaptability to climate variability by improving dehydration efficiency. This may provide some resilience in regions with unpredictable weather, such as unexpected rainfall or humidity during harvest. Hybrids with faster dehydration rates reduce the risk of spoilage under humid conditions, enabling greater flexibility in harvest timing and preserving grain quality without immediate drying interventions. In an era of increasing climate extremes, such resilient hybrids can stabilize yields and support food security, offering a proactive strategy to build adaptable agricultural systems capable of meeting future demands.

The identification of consistent QTLs and the discovery of candidate genes offer promising targets for MAS. These genetic insights provide a basis for developing maize varieties that may be better suited for mechanized harvesting by potentially reducing GMC at harvest and increasing dehydration rates. Future research should focus on the functional validation of these candidate genes and their incorporation into breeding programs. By leveraging these genetic insights, breeders can develop maize varieties that not only meet the demands of modern agriculture but also contribute to more sustainable and efficient production systems. Nonetheless, the successful translation of these findings into breeding applications will depend on continued research, validation, and optimization within real-world agricultural settings.

Conclusions

In this study, we developed a recombinant inbred line (RIL) population and constructed a corresponding genetic linkage map that spans 1237.36 cM and includes 5235 bin markers using the Genotyping-by-Sequencing (GBS) approach. This map was used to evaluate grain moisture content (GMC) and grain dehydration rate (GDR) across three distinct environments at three developmental stages. A total of 23 QTLs for GMC and AUDDC were identified, distributed across chromosomes 1, 2, 5, 6, 9, and 10, with several QTLs accounting for more than 10% of the phenotypic variance. Notably, significant QTLs such as *qGMC1.1*, qGMC2.2, and *qAUDDC2.2* were consistently detected across various environments and developmental stages. Transcriptomic analysis revealed 21 candidate genes within these QTL regions, including transcription factors, metabolism-related genes, and others. These findings provide insights into the genetic basis of GMC and GDR, may contribute to the development of marker-assisted selection strategies in maize breeding. However, further validation is needed to confirm the stability and effectiveness of the identified loci across different genetic backgrounds and environmental conditions before their potential application in improving mechanized production efficiency.

Abbreviations

GMC	Grain moisture content
GDR	Grain dehydration rate
QTL	Quantitative trait loci
AUDDC	Area under the dry down curve
RIL	Recombinant inbred line
DAP	Days after pollination

Supplementary Information

The online version contains supplementary material available at https://doi.org/10.1186/s12870-025-06404-1.

Supplementary Material 1

Acknowledgements

The authors are grateful to Research Fellow Chunmiao Li (Dancheng Institute of Agricultural Science) for field management. we also extend our sincere thanks to all the reviewers who contributed their tome and expertise to the review process.

Author contributions

Conceptualization, Y.D. and J.Z.; methodology, J.Z.; software, F.Z. and Y.F.; formal analysis, Y.Z.; L.T. and Q.Z.; investigation, Y.Z.; X.W. and Q.Z.; visualization, Z.M. and X.M.; writing—original draft preparation, J.Z.; writing—review and editing, L.T.; project administration, L.X.; funding acquisition, Q.Z. and Y.D.; All authors read and approved the final manuscript.

Funding

This work was supported by grants from National Key Research and Development Program of China (2021YFD1200700); Special Project of Science and Technology Innovation Team of Henan Academy of Agricultural Sciences (2024TD40), Project of Corn Industry Technology System Construction in Henan (HARS-22-02-G2); Special Fund for Independent Innovation of Henan Academy of Agricultural Science (2023ZC008).

Data availability

All data generated or analyzed during this study are included in this article and its supplementary information files or are available from the corresponding author on reasonable request. RNA sequencing data have been deposited in the National Center for Biotechnology Information's Sequence Read Archive (NCBI SRA) under accession number PRJNA1166843.

Declarations

Ethics approval and consent to participate

Not applicable.

Consent for publication

Not applicable.

Competing interests

The authors declare no competing interests.

Received: 29 September 2024 / Accepted: 13 March 2025
Published online: 21 March 2025

References

1. Parvej MR, Hurburgh CR, Hanna HM, Licht MA. Dynamics of corn dry matter content and grain quality after physiological maturity. Agron J. 2020;112(2):998–1011.
2. Capelle V, Remoué C, Moreau L, Reyss A, Mahé A, Massonneau A, et al. QTLs and candidate genes for desiccation and abscisic acid content in maize kernels. BMC Plant Biol. 2010;10:2.
3. Huang Z, Xue J, Ming B, Wang K, Xie R, Hou P, et al. Analysis of factors affecting the impurity rate of mechanically-harvested maize grain in China. Int J Agricultural Biol Eng. 2020;13(5):17–22.
4. Li W, Yu Y, Wang L, Luo Y, Peng Y, Xu Y, et al. The genetic architecture of the dynamic changes in grain moisture in maize. Plant Biotechnolo J. 2021;19(6):1195–205.
5. Yin S, Liu J, Yang T, Li P, Xu Y, Fang H, et al. Genetic analysis of the seed dehydration process in maize based on a logistic model. Crop J. 2020;8(2):182–93.
6. Sala RG, Andrade FH, Camadro EL, Cerono JC. Quantitative trait loci for grain moisture at harvest and field grain drying rate in maize (*Zea mays*, L). Theor Appl Genet. 2006;112(3):462–71.
7. Rodrigues DM, Coradi PC, Teodoro LPR, Teodoro PE, Moraes RDS, Leal MM. Monitoring and predicting corn grain quality on the transport and post-harvest operations in storage units using sensors and machine learning models. Sci Rep. 2024;14(1):6232.
8. Chase SS. Relation of yield and number of days from planting to flowering in early maturity maize hybrids of equivalent grain moisture at harvest[2]. Crop Sci. 1964;4(1):111–2.
9. Cross HZ. A selection procedure for ear drying-rates in maize. Euphytica. 1985;34:409–18.
10. Li S, Zhang C, Yang D, Lu M, Qian Y, Jin F, et al. Detection of QTNs for kernel moisture concentration and kernel dehydration rate before physiological maturity in maize using multi-locus GWAS. Sci Rep. 2021;11(1):1764.
11. Liu J, Yu H, Liu Y, Deng S, Liu Q, Liu B, et al. Genetic dissection of grain water content and dehydration rate related to mechanical harvest in maize. BMC Plant Biol. 2020;20(1):118.
12. Austin DF, Lee M, Veldboom LR, Hallauer AR. Genetic mapping in maize with hybrid progeny across testers and generations: grain yield and grain moisture. Crop Sci. 2000;40:30–9.
13. Li Y, Dong Y, Yang M, Wang Q, Shi Q, Zhou Q, et al. QTL detection for grain water relations and genetic correlations with grain matter accumulation at four stages after pollination in maize. J Plant Biochem Physiol. 2014;2:1.
14. Kebede AZ, Woldemariam T, Reid LM, Harris LJ. Quantitative trait loci mapping for gibberella ear rot resistance and associated agronomic traits using genotyping-by-sequencing in maize. Theor Appl Genet. 2016;129(1):17–29.
15. Song W, Shi Z, Xing J, Duan M, Su A, Li C, et al. Molecular mapping of quantitative trait loci for grain moisture at harvest in maize. Plant Breed. 2017;136:28–32.
16. Zhang J, Zhang F, Tang B, Ding Y, Xia L, Qi J, et al. Molecular mapping of quantitative trait loci for grain moisture at harvest and field grain drying rate in maize (*Zea mays*, L). Physiol Plant. 2020;169:64–72.
17. Wang Z, Wang X, Zhang L, Liu X, Di H, Li T, et al. QTL underlying field grain drying rate after physiological maturity in maize (*Zea Mays* L). Euphytica. 2012;185:521–8.
18. Cui Z, Dong H, Zhang A, Ruan Y, Jiang S, He Y, et al. Denser markers and advanced statistical method identified more genetic loci associated with husk traits in maize. Sci Rep. 2020;10:8165.
19. Jia T, Wang L, Li J, Ma J, Cao Y, Lübberstedt T, et al. Integrating a genome-wide association study with transcriptomic analysis to detect genes controlling grain drying rate in maize (*Zea may*, L). Theor Appl Genet. 2020;133:623–34.
20. Liu Y, Ao M, Lu M, Zheng S, Zhu F, Ruan Y et al. Genomic selection to improve husk tightness based on genomic molecular markers in maize. Front Plant Sci. 2023;14.
21. Zhang J, Zhang F, Tian L, Ding Y, Qi J, Zhang H et al. Molecular mapping of quantitative trait loci for 3 husk traits using genotyping by sequencing in maize (*Zea mays* L.). G3 (Bethesda, Md.), 2022;12(10):jkac198.
22. Dong Y, Feng Z, Ye F, Li T, Li G, Li Z-S, et al. Genome-wide association analysis for grain moisture content and dehydration rate on maize hybrids. Mol Breed. 2023;43(1):5.
23. Alvarado G, Rodríguez FM, Pacheco A, Burgueño J, Crossa J, Vargas M, et al. META-R: A software to analyze data from multi-environment plant breeding trials. Crop J. 2020;8(5):745–56.
24. Li H, Durbin R. Fast and accurate short read alignment with Burrows-Wheeler transform. Bioinf (Oxford England). 2009;25(14):1754–60.
25. Li H, Handsaker B, Wysoker A, Fennell T, Ruan J, Homer N, et al. The sequence alignment/map format and samtools. Bioinf (Oxford England). 2009;25(16):2078–9.
26. Wang K, Li M, Hakonarson H. ANNOVAR: functional annotation of genetic variants from high-throughput sequencing data. Nucleic Acids Res. 2010;38(16):e164.
27. Xie W, Feng Q, Yu H, Huang X, Zhao Q, Xing Y, et al. Parent-independent genotyping for constructing an ultrahigh-density linkage map based on population sequencing. Proc Natl Acad Sci U S A. 2010;107(23):10578–83.

28. Meng L, Li H, Zhang L, Wang J. QTL icimapping: integrated software for genetic linkage map construction and quantitative trait locus mapping in biparental populations. Crop J. 2015;3(3):269–83.
29. Wu Y, Zhou Z, Dong C, Chen J, Ding J, Zhang X, et al. Linkage mapping and genome-wide association study reveals Conservative QTL and candidate genes for fusarium rot resistance in maize. BMC Genomics. 2020;21:357.
30. Zhou G, Mao Y, Xue L, Chen G, Lu H, Shi M, et al. Genetic dissection of husk number and length across multiple environments and fine-mapping of a major-effect QTL for husk number in maize (*Zea Mays* L). Crop J. 2020;8:1071–80.
31. Liu Y, Wang L, Sun C, Zhang Z, Zheng Y, Qiu F. Genetic analysis and major QTL detection for maize kernel size and weight in multi-environments. Theor Appl Genet. 2014;127:1019–37.
32. Brooking IR. Maize ear moisture during grain-filling, and its relation to physiological maturity and grain-drying. Field Crops Res. 1990;23(1):55–68.
33. Dong Y, Feng ZQ, Ye F, et al. Genome-wide association analysis for grain moisture content and dehydration rate on maize hybrids. Mol Breed. 2023;43(1):5.
34. Xu Y, Crouch JH. Marker-assisted selection in plant breeding: from publications to practice. Crop Sci. 2008;48(2):391.
35. Shiferaw B, Prasanna BM, Hellin J, Bänziger M. Crops that feed the world 6. Past successes and future challenges to the role played by maize in global food security. Food Secur. 2011;3(3):307–27.
36. Geng L, Zhang W, Zou T, Du Q, Ma X, Cui D, et al. Integrating linkage mapping and comparative transcriptome analysis for discovering candidate genes associated with salt tolerance in rice. Front Plant Sci. 2023;14:1065334.
37. Mihaljevic R, Schön CC, Utz HF, Melchinger AE. Correlations and QTL correspondence between line per se and testcross performance for agronomic traits in four populations of European maize. Crop Sci. 2005;45(1):114–22.
38. Sala RG, Andrade FH, Cerono JC. Quantitative trait loci associated with grain moisture at harvest for line per se and testcross performance in maize: a meta-analysis. Euphytica. 2012;185(3):429–40.
39. Zhang C, Zhou Z, Yong H, Zhang X, Hao Z, Zhang F, et al. Analysis of the genetic architecture of maize ear and grain morphological traits by combined linkage and association mapping. Theor Appl Genet. 2017;130(5):1011–29.
40. Yin S, Li P, Xu Y, Liu J, Yang T, Wei J, et al. Genetic and genomic analysis of the seed-filling process in maize based on a logistic model. Heredity (Edinb). 2020;124:122–34.
41. Kang MS, Zuber MS, Horrocks RD. An electronic probe for estimating ear moisture content of maize[1]. Crop Sci. 1978;18:1083–4.
42. Freppon JT, St. Martin SK, Pratt RC, Henderlong PR. Section for low ear moisture in corn, using a Hand-Held meter. Crop Sci. 1992;32(4):1062–4.
43. Yang J, Carena MJ, Uphaus J. Area under the dry down curve (AUDDC): A method to evaluate rate of dry down in maize. Crop Sci. 2010;50:2347–54.
44. Reid LM, Morrison MJ, Zhu X, Wu J, Wolde T, Volovaca C, et al. Selecting maize for rapid kernel drydown: timing of moisture measurement. Maydica. 2014;59:9–15.
45. Qian YL, Zhang XQ, Wang LF, Chen J, Chen BR, Lv GH, et al. Detection of QTLs controlling fast kernel dehydration in maize (*Zea Mays* L). Genet Mol Res. 2016;15(3). https://doi.org/10.4238/gmr.15038151.
46. Li S, Zhang C, Lu M, Yang D, Qian Y, Yue Y, et al. QTL mapping and GWAS for field kernel water content and kernel dehydration rate before physiological maturity in maize. Sci Rep. 2020;10(1):13114.
47. Wang W, Ren Z, Li L, Du Y, Zhou Y, Zhang M, et al. Meta-QTL analysis explores the key genes, especially hormone related genes, involved in the regulation of grain water content and grain dehydration rate in maize. BMC Plant Biol. 2022;22(1):346.
48. Qu J, Xu S, Gou X, Zhang H, Cheng Q, Wang X, et al. Time-resolved multiomics analysis of the genetic regulation of maize kernel moisture. Crop J. 2023;11(1):247–57.
49. Andriankaja A, Boisson-Dernier A, Frances L, et al. AP2-ERF transcription factors mediate Nod factor dependent Mt ENOD11 activation in root hairs via a novel cis-regulatory motif. Plant Cell. 2007;19(9):2866–85.
50. Aghdam MS, Luo Z, Jannatizadeh A, Sheikh-Assadi M, Sharafi Y, Farmani B, et al. Employing exogenous melatonin applying confers chilling tolerance in tomato fruits by upregulating ZAT2/6/12 giving rise to promoting endogenous polyamines, proline, and nitric oxide accumulation by triggering arginine pathway activity. Food Chem. 2019;275:549–56.
51. Xu H, Li Z, Tong Z, He F, Li X. Metabolomic analyses reveal substances that contribute to the increased freezing tolerance of alfalfa (*Medicago sativa* L.) after continuous water deficit. BMC Plant Biol. 2020;20:15.
52. Ding Z, Millar AJ, Davis AM, Davis SJ. TIME FOR COFFEE encodes a nuclear regulator in the Arabidopsis Thaliana circadian clock. Plant Cell. 2007;19(5):1522–36.
53. Weiss J, Terry MI, Martos-Fuentes M, Letourneux L, Ruiz-Hernández V, Fernández JA, et al. Diel pattern of circadian clock and storage protein gene expression in leaves and during seed filling in Cowpea (Vigna unguiculata). BMC Plant Biol. 2018;18(1):33.
54. Du XF, Li FN, Peng XL, Xu B, Zhang Y, Li G, et al. Circadian regulation of developmental synaptogenesis via the hypocretinergic system. Nat Commun. 2023;14(1):3195.
55. Shi W, Shao H, Sha Y, Shi R, Shi D, Chen Y, et al. Grain dehydration rate is related to post-silking thermal time and ear characters in different maize hybrids. J Integr Agric. 2022;21:964–76.

Publisher's note